

## Adsorption and Activity of a Domoic Acid Binding Antibody Fragment on Mesoporous Silicates

Xuejun Hu,<sup>†</sup> Stefania Spada,<sup>†,‡</sup> Simon White,<sup>†,‡</sup> Sarah Hudson,<sup>†,‡</sup> Edmond Magner,<sup>†,‡</sup> and J. Gerard Wall<sup>\*,†,‡</sup>

Department of Chemical and Environmental Sciences, and Materials and Surface Science Institute, University of Limerick, Plassey Technology Park, Limerick, Ireland

Received: April 20, 2006; In Final Form: July 31, 2006

The adsorption of an anti-domoic acid single-chain Fv (scFv) antibody fragment onto a range of mesoporous silicate supports was investigated. The scFv fragment adsorbed to all materials investigated, and *pI* had an apparently large effect on coating, with the greatest—and fastest—adsorption found on the most negatively charged silicates. Maximal coating levels attainable did not reflect the pore diameters of the materials. The immobilized antibody was functional on all materials and bound its antigen, a naturally occurring neurotoxin produced by shellfish, in a rapidly saturating manner that suggested the antibody adsorbed in a multilayer on the mesoporous particles. The antigen:antibody ratio decreased from 1:1.3 to <1:10 with increasing concentration of immobilized antibody, and the immobilized scFv exhibited no detectable reduction in domoic acid binding over a 42-day incubation period.

### Introduction

Mesoporous silicates (MPS), such as those synthesized using a liquid crystal templating mechanism, have been investigated as support materials for organic molecules since their original discovery.<sup>1,2</sup> They have highly ordered pore structures and tight pore size distributions,<sup>3</sup> with surface areas as large as 1000 m<sup>2</sup>/g. They are chemically and mechanically stable due to their inorganic silicate framework, and it is now increasingly possible to tailor their pore size during synthesis to accommodate specific biomolecules. Furthermore, their surfaces can be modified with a variety of functional groups to promote, e.g., protein adsorption, so they have potential application in separation technologies,<sup>4</sup> biocatalysis,<sup>5</sup> and biosensors.<sup>6</sup>

Single-chain Fv (scFv) antibody fragments are recombinant molecules consisting of antibody heavy chain and light chain variable regions, which together form the antigen binding pocket of an antibody molecule, connected by a synthetic peptide linker.<sup>7</sup> They are the smallest antibody fragments comprising an intact antigen-binding site and, thus, are capable of retaining the binding properties of their parent antibodies. Their significantly reduced size relative to whole antibodies (~28 kDa vs ~146 kDa) is a significant advantage in tumor therapy,<sup>8</sup> due to improved tumor penetration and more rapid clearance from the body, and in immunosensor development,<sup>9</sup> where binding sites can be more densely packed onto solid supports.

We have previously reported the cloning and production of a recombinant scFv against domoic acid.<sup>10</sup> Domoic acid is a naturally occurring amino acid which acts as a potent neurotoxin in humans, causing amnesic shellfish poisoning.<sup>11,12</sup> It is produced by species of the diatom genus *Pseudo-nitzschia*, and it accumulates in filter-feeding shellfish during algal blooms.<sup>13,14</sup> It has been detected in a variety of shellfish throughout the

world, and ingestion of contaminated shellfish can lead to death in severe cases.<sup>15–17</sup> Marine animals are also affected.<sup>18–20</sup>

The availability of an analytical test to detect domoic acid in shellfish and seawater is critical to minimizing human exposure. The E.U.-defined regulatory limit for safety of consumers is 20 µg/g of shellfish, while the U.S. FDA advises a limit of 20 ppm (20 µg/g) in shellfish and 30 ppm in crabs.<sup>21</sup> The methods used routinely to enforce the limits are mouse bioassays<sup>22</sup> and HPLC-based tests.<sup>23–26</sup> Such methods are unsuitable for large-scale or in situ screening, however, as they are expensive and time- and equipment-intensive. Immunological methods have also been developed, and these offer the advantage of being cheaper and less time-consuming, while still sufficiently sensitive to meet regulatory requirements.<sup>27,28</sup> Recently, disposable electrochemical immunosensors have been reported in which an indirect competitive, monoclonal antibody based immunoassay occurs on the carbon working surface of a screen-printed electrode.<sup>29,30</sup>

In this study, we investigate the use of mesoporous silicate materials in the development of biosensors for in situ environmental screening. The anti-domoic acid scFv is adsorbed onto a range of MPS materials of differing physicochemical properties, and the stability of the immobilized scFv and its ability to detect domoic acid is determined.

### Experimental Section

**Materials.** Tetramethylammonium hydroxide (TMAOH, 97%), 1,2-bis(trimethoxysilyl)ethane (BTMSE, 96%), and trimethylbenzene (TMB, 97%) were obtained from Sigma-Aldrich. Fumed silica (SiO<sub>2</sub>), methanol (CH<sub>3</sub>OH, 99.9%), ethanol (C<sub>2</sub>H<sub>5</sub>OH, 99.0%), and ammonium hydroxide (NH<sub>3</sub>, 33%) were obtained from Fluka (Riedel de Haën). Tetraethoxysilane (TEOS, 98%), cetyltrimethylammonium bromide (CTAB, 99%), and 2-cyanoethyltriethoxysilane (CEOS, 97%) were purchased from Lancaster. Pluronic-P123 (EO20PO70EO20) was obtained as a gift from BASF. Hydrochloric acid (HCl, 37%) was

\* Corresponding author. Telephone: 353-61-202296. Fax: 353-61-202568. E-mail: gerard.wall@ul.ie.

<sup>†</sup> Department of Chemical and Environmental Sciences.

<sup>‡</sup> Materials and Surface Science Institute.

obtained from BDH laboratory supplies. Water was purified (18.2 M $\Omega$ ) using an Elgastat SPECTRUM system. Domoic acid was obtained from Sigma-Aldrich. *Escherichia coli* (*E. coli*) TOP10 bacterial cells (F' *mcrA*  $\Delta$ (*mrr-hsdRMS-mcrBC*)  $\Phi$ 80lacZ $\Delta$ M15  $\Delta$ lacX74 *deoR recA1 araD139*  $\Delta$ (*ara-leu*)7697 *galU galK rpsL* (Str<sup>R</sup>) *endA1 nupG*; Invitrogen Corp.) and the periplasmic expression vector pIG6<sup>31</sup> were used for protein production.

### Synthesis and Characterization of Mesoporous Materials.

The mesoporous silicates SBA-15,<sup>32</sup> CNS,<sup>3,33</sup> MSE,<sup>34,35</sup> and MCM-41/80<sup>1,36</sup> were synthesized according to published methods. For SBA-15, a nonionic triblock copolymer P-123 was used as a templating agent with TEOS as the silica source in an acidified solution. For CNS (cyano functionalized silica), the cationic surfactant CTAB was used as the templating agent with a combination of TEOS and CEOS in a basic medium. For MCM-41/80, CTAB with the addition of the swelling agent TMB was used as the templating agent, with fumed silica as the silica source and TMAOH provided as a basic medium. After synthesis the organic templates were removed from the three materials by Soxhlet extraction using ethanol followed by calcination at 550 °C for CNS and MCM-41/80, and 500 °C for SBA-15. For MSE (periodic mesoporous organosilica), an SBA-15 type synthesis was used with a lower acid content and the addition of BTMSE. The organic templates were removed from this material and the uncalcined sample of CNS by repeated Soxhlet extractions using ethanol.

All of the silicates used were characterized by nitrogen gas adsorption/desorption isotherms at 77 K measured using a Micromeritics Gemini ASAP 2010 system. Samples were pretreated by heating to 423 K for 12 h under vacuum (348 K in the case of MSE). The pore size data were analyzed by the thermodynamic-based Barrett–Joyner–Halenda (BJH) method<sup>37</sup> using the desorption branch of the isotherm, and surface areas were measured using the Brunauer–Emmett–Teller (BET) method.<sup>38</sup> The mesopore volume was estimated from the volume of nitrogen adsorbed after the micropores had been filled until condensation into the mesopores was complete.

Isoelectric points and zeta ( $\zeta$ ) potentials were determined using a Malvern 2000 Zeta sizer. Samples of MPS materials were prepared in deionized water (18.2 M $\Omega$ ; Elgastat) at 20 mg/200 mL and sonicated for 15 min. HCl (0.1 M) was added dropwise to 50 mL aliquots until pH 2.0 was reached, while 0.1 M NaOH was added dropwise to similar aliquots up to pH 8.0.  $\zeta$ -potential measurements were determined (in triplicate, standard deviation of 5%) at each point, and isoelectric points were calculated using the system software.

### Expression and Purification of scFv Antibody Fragment.

The antibody V<sub>H</sub> and V<sub>L</sub> variable regions were isolated from the 2H12 mouse hybridoma cell line as described previously.<sup>10</sup> These were combined in a V<sub>H</sub>–linker–V<sub>L</sub> scFv with a (Gly<sub>4</sub>–Ser)<sub>3</sub> interdomain linker and a C-terminal His<sub>6</sub> tag for purification. The scFv was produced in *E. coli* TOP10 cells using the periplasmic expression vector pIG6,<sup>31</sup> while the *dsbC* gene, encoding *E. coli* disulfide bond isomerase C enzyme, was coexpressed from the vector to increase antibody production.<sup>10</sup> Following antibody production for 8 h at 25 °C, soluble proteins were prepared from the 1-L culture and applied to a His Trap nickel affinity column (Amersham), according to the manufacturer's instructions, but with the addition of 2% Tween-20 to the sample prior to column loading. Elution was carried out in the presence of 500 mM imidazole, and eluted fractions were analyzed by SDS–PAGE on 12% acrylamide gels and Western blotting.

**Adsorption of scFv to Mesoporous Supports.** Adsorption of the scFv antibody fragment to mesoporous materials was carried out by mixing 0.5 mL of an scFv solution (final concentration 0.5–5.0  $\mu$ M in 10 mM phosphate-buffered saline (PBS) buffer, pH 7.4) and 0.5 mL of the mesoporous silicate solution (final concentration 1 mg/mL in the same buffer). The suspension was incubated with rocking for 1–80 h at 25 °C, followed by centrifugation at 12 000 rpm for 5 min to pellet the silicate material and measurement of absorbance at 280 nm of the scFv-containing supernatant. The concentration of antibody fragment in the supernatant was determined from the absorbance at 280 nm using a standard curve prepared with purified scFv, and the amount of antibody adsorbed to silicate samples was calculated by determining the difference in the amount of scFv in solution before and after adsorption to the silicates. Following adsorption, the silicates were washed five times with PBS buffer and the adsorbed antibody values were corrected for the washing.

**Measurement of Domoic Acid Binding.** Following adsorption of the 2H12 scFv at concentrations ranging from 0.5 to 5  $\mu$ M, the silicates were washed five times with PBS and 1–5  $\mu$ g/mL domoic acid in PBS buffer, pH 7.4, was added. The suspension was incubated, with rolling, for 20 h at 25 °C, following which samples were centrifuged at 12 000 rpm for 5 min and the OD<sub>260</sub> of the supernatant was measured. The concentration of domoic acid in the supernatant was determined using a standard curve, and the domoic acid binding by the antibody fragment was calculated by subtraction from the original domoic acid concentration. The amount of bound domoic acid was corrected for binding to the silicates, which was always less than 4% of binding by the immobilized antibody.

In analysis of stability of domoic acid binding on the silicate supports, adsorbed antibody–silicate suspensions were stored at 4 °C for up to 42 days following scFv adsorption, before performing the binding to domoic acid.

## Results and Discussion

**Characterization of the Mesoporous Materials.** In this study, five previously characterized mesoporous materials—SBA-15,<sup>32</sup> MCM-41/80,<sup>1</sup> a cyano functionalized silicate (CNS),<sup>3</sup> CNScal (calcined CNS), and MSE,<sup>34,35</sup> in which ethylene is interspersed into the framework of the silicate—were used as supports for immobilization of an anti-domoic acid scFv antibody fragment.

Surface areas and pore size were determined for each of the silicates used (Table 1). SBA-15, MCM-41/80, and MSE have average pore diameters of 70, 80, and 62 Å, respectively; also, SBA-15 and MSE have very tight pore size distributions due to their highly ordered pore structures. Based on solved structures in the Research Collaboratory for Structural Bioinformatics (RCSB) data bank, scFv antibody fragments have dimensions on the order of 50 Å by 40 Å by 40 Å, so scFv molecules should be sufficiently small to enter the pores of these silicates. CNS materials, meanwhile, have pore diameters considerably greater than that of the antibody fragment (Table 1).

While each of the materials offers a very large surface area that is ideal for adsorption, the total surface area of each silicate was calculated to verify that the materials were sufficiently large to allow monolayer coating of the scFv at the protein concentrations used. The 2H12 scFv antibody fragment dimensions were taken as average scFv antibody fragment dimensions, as outlined above, based on which a theoretical monolayer of adsorbed scFv

**TABLE 1: Physicochemical Characteristics of the Different Mesoporous Silicates<sup>a</sup>**

material	surface area (m <sup>2</sup> /g)	C <sub>BET</sub>	pore size distribution (Å)	average pore diameter (Å)	pI
SBA-15	415	109	60–95	70	3.5
CNS	338	50	150–400	240	4.5
CNScal	533	66	90–240	190	4.8
MCM-41/80	678	107	30–180	80	3.5
MSE	1223	106	55–75	62	5.2

<sup>a</sup> Surface area, pore size distribution, and average pore diameter were obtained from nitrogen adsorption/desorption analysis. Isoelectric points were calculated using a Malvern 2000 Zeta sizer.

**TABLE 2: Surface Areas and Volumes of the Mesoporous Materials and Theoretical Amounts of Each Occupied by Adsorbed scFv at Different Concentrations**

material	surface area MPS (m <sup>2</sup> /g)	mesopore volume <sup>a</sup> (cm <sup>3</sup> /g)	scFv (μmol/g)	theor surface occupied by scFv <sup>b</sup> (m <sup>2</sup> /g)	% theor surface occupied by scFv <sup>b</sup>	% theor mesopore vol occupied by scFv <sup>b</sup>
SBA-15	415	0.47	1.0	17.0	4.1	14.5
			2.5	42.6	10.3	36.2
			5.0	85.2	20.5	72.5
			10.0	170.4	41.0	145.0
CNS	338	1.40	1.0	17.0	5.0	4.9
			2.5	42.6	12.6	12.2
			5.0	85.2	25.2	24.3
			10.0	170.4	50.4	48.6
CNScal	533	1.23	1.0	17.0	3.2	5.5
			2.5	42.6	8.0	13.9
			5.0	85.2	16.0	27.7
			10.0	170.4	32.0	55.4
MCM-41/80	678	1.26	1.0	17.0	2.5	5.4
			2.5	42.6	6.3	13.5
			5.0	85.2	12.6	27.0
			10.0	170.4	25.2	54.0
MSE	1223	0.80	1.0	17.0	1.4	8.6
			2.5	42.6	3.5	21.3
			5.0	85.2	7.0	42.6
			10.0	170.4	14.0	85.2

<sup>a</sup> Volume of liquid nitrogen at STP. <sup>b</sup> Theoretical surface/volume occupied by scFv.

was calculated to cover from 1.4% (1 μmol/g scFv on MSE) to 25.2% (5 μmol/g on CNS) of the surface area of the materials (Table 2). The relatively large mesopore volumes of CNS and CNScal result from their large pore sizes, while MCM-41/80 has a highly ordered hexagonal structure,<sup>3</sup> leading to a significantly larger mesopore volume than SBA-15 and MSE, which also have average pore diameters similar to the size of the scFv molecule.

The ζ-potential of each material was determined as a function of pH, resulting in isoelectric point (pI) values of 3.5 for MCM-41/80 and SBA-15, 4.5 for CNS, 4.8 for CNScal, and 5.2 for MSE (Table 1). In addition, Figure 1 reveals a more shallow curve in the ζ-potential profile of MSE than the other materials, leading to a ζ-potential for MSE of −11 mV at the pH (7.4) at which the experiments were carried out. The other four materials, however, show ζ-potentials from −35 to −40 mV at pH 7.4 and are thus more negatively charged than MSE in scFv adsorption studies, despite their similar pI values.

**Adsorption of scFv onto Mesoporous Materials.** The mesoporous materials used in this study were selected based on their pore sizes, with average diameters that range from slightly larger (MSE, SBA-15, and MCM-41/80) to approximately 3–5 times greater (CNS, CNScal) than that of the scFv molecule. The purified scFv antibody (1 μM) was allowed to adsorb onto 1 mg/mL of each mesoporous material over 80 h. SBA-15 and MCM-41/80 exhibited the fastest rate of adsorption, with adsorption 96–97% complete after 2 h and maximal loading reached after 3 h (Figure 2). CNS and CNScal showed slightly slower rates of adsorption, with adsorption 93% and 91% complete, respectively, after 2 h, and 3 and 5 h required to reach saturation, respectively, but with the same amount of total adsorbed scFv achieved as for SBA-15 and MCM-41/80. Meanwhile, antibody adsorption to MSE, which has the smallest pore sizes of all the materials, occurred at a significantly slower

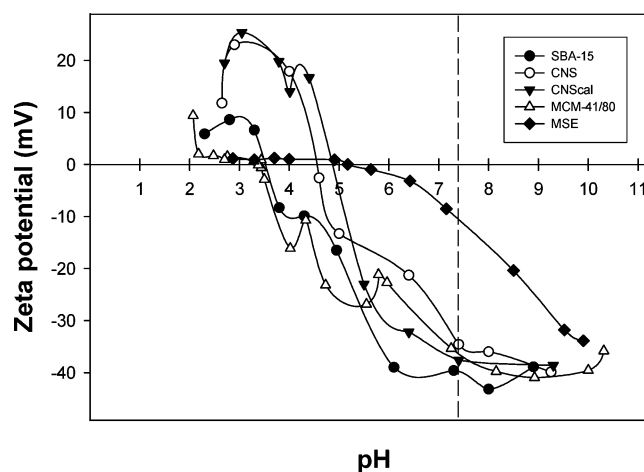


**Figure 1.** ζ-potentials plotted against pH for mesoporous materials. ζ-potentials were determined from triplicate samples after sonication. The dotted line indicates pH 7.4, at which adsorption experiments were carried out.

rate than to the other silicates (44% complete after 2 h, maximal loading after 10 h) and reached saturation with a lower amount of adsorbed scFv, though this most likely reflects a weak electrostatic interaction between MSE and the scFv, as discussed below.

Adsorption isotherms were also generated for each of the mesoporous materials by incubating various concentrations of the scFv with the materials for 20 h at 25 °C. SBA-15, MCM-41/80, and CNS were observed to have the strongest affinity for the scFv, with CNScal exhibiting an intermediate behavior and MSE a weaker interaction than the other materials, as shown in Figure 3. While the isotherms in Figure 3 have clearly not reached a plateau, it was not possible to saturate the mesoporous



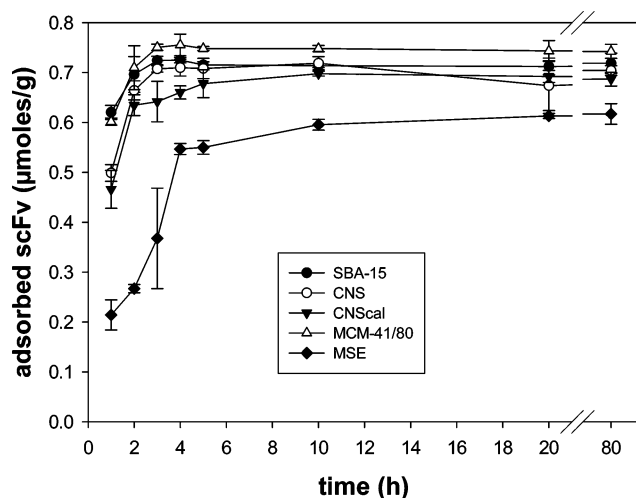


**Figure 2.** Adsorption of scFv onto mesoporous materials over time. Error bars represent standard deviations obtained from triplicate samples. The initial scFv concentration was 1  $\mu\text{mol/g}$  for all silicates, and adsorption was carried out at pH 7.4.

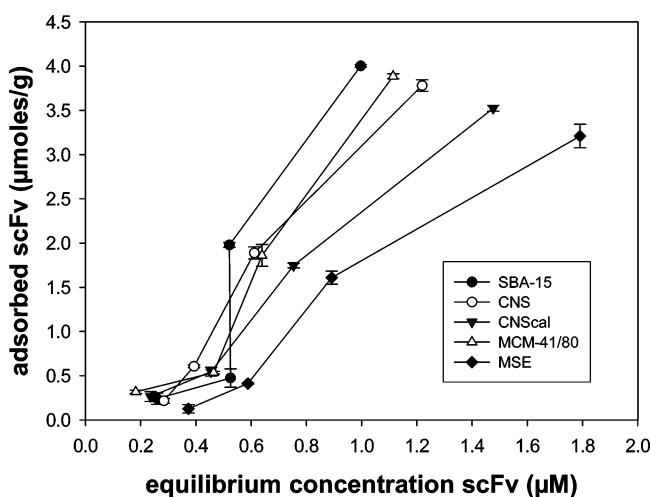


**Figure 3.** Adsorption isotherms for scFv onto different mesoporous materials. Error bars represent standard deviations obtained from triplicate samples.

materials in this analysis as the purified antibody fragment underwent aggregation in solution at concentrations greater than 5  $\mu\text{M}$ , which corresponds to equilibrium solution concentrations of 1.0  $\mu\text{M}$  (SBA-15) to 1.8  $\mu\text{M}$  (MSE).

The amount of antibody adsorbed to each material ranged from 80% of the scFv incubated with SBA-15, to 77% for MCM-41/80, 75% for CNS, 70% for CNScal, and only 64% for MSE. This corresponds to an scFv adsorption capacity ranging from 90 mg/g (onto MSE) to 112 mg/g (onto SBA-15). This antibody fragment loading represents only 4.5–19.1% of the theoretical total surface area available for adsorption, however, while it also shows surprisingly little variation between the materials given their broad ranges of pore diameters (62–240 Å; Table 1) and mesopore volumes (0.47–1.4  $\text{cm}^3/\text{g}$ ; Table 2). The low coverage of the silicates may indicate that the scFv molecules adsorb to the materials at or close to the mesopore entrance, leading to multilayer protein adsorption.<sup>39,40</sup> Extensive characterization of the adsorption of cytochrome *c* to CNS, CNScal, and MCM-41 previously demonstrated that cytochrome *c* exhibited increased adsorption to materials as the pore diameter was increased from smaller than the protein to only 3-fold larger

than the protein's molecular diameter, because of the greater (mesopore) surface area accessible to the protein for adsorption.<sup>39</sup>

Investigation of the *pI* of the scFv fragment and silicate materials found a greater correlation with antibody adsorption. The scFv has a theoretical *pI* of 8.73, and is therefore expected to be positively charged at pH 7.4, at which the experiments were carried out. Meanwhile, the silicates have *pI* values ranging from 3.5 to 5.2. The scFv adsorbed most strongly to MCM-41/80 (*pI* 3.5) and SBA-15 (*pI* 3.5), followed by CNS (*pI* 4.5) and CNScal (*pI* 4.8), and then much more weakly to MSE (*pI* 5.2; Figures 2 and 3). While the *pI* of MSE is higher than that of the other materials, it also has a significantly less negative  $\zeta$ -potential at pH 7.4 (−11 mV; Figure 1) than the other four materials (−35 to −40 mV) and so is less negatively charged under experimental conditions, resulting in a weaker electrostatic interaction with the scFv. Suh and co-workers<sup>41</sup> also found decreased adsorption capacity of BSA on a silica surface as the pH was increased above the *pI* of BSA, leading to a repulsive force between the BSA and the silica surface, while a close correlation between the isoelectric point of a number of proteins and their adsorption onto CNS has also been reported.<sup>39</sup> Furthermore, adsorption studies with cytochrome *c* and xylanase on MSE and SBA-15 found that not only the adsorption capacity, but also the rate of protein adsorption, increased dramatically when proteins and support materials had opposite charges,<sup>35</sup> so it seems likely that differing electrostatic interaction strengths, resulting from *pI* differences between the silicates, are the main reason for the differing adsorption characteristics of these mesoporous materials.

The interaction of the scFv antibody fragment on the mesoporous silicate materials was assessed by washing scFv–silicate samples with 10% poly(ethylene glycol) (PEG) and quantifying the protein thus removed. Following adsorption of 5  $\mu\text{M}$  scFv to the silicate support materials, washing in PEG led to removal of 4% of adsorbed scFv from MSE, followed by 6.2% from SBA-15, 7.2% from MCM-41/80, and 8.5% and 8.9% from CNS and CNScal, respectively. The low level of scFv desorbed with PEG, coupled with the observation that *pI* has a critical role in determining antibody adsorption, suggests that the interaction between the antibody fragment and silicates is mostly charge related.

**Stability.** As one of the primary parameters to be considered in immunosensor development is the stability of the analyte in the biological matrix, the materials that performed best in adsorption studies, SBA-15 and MCM-41/80, were also incubated with adsorbed scFv in PBS at 4  $^{\circ}\text{C}$  over 42 days to measure the stability of the immobilized scFv. No leaching of the scFv was detectable over the test period, which confirmed that the adsorbed scFv is tightly bound to the silicates and that the silicates could be used for up to 6 weeks after coating with antibody. Other workers have found that screen-printed electrodes with immobilized anti-domoic acid antibody showed a significant drop in signal after 15 days at 4  $^{\circ}\text{C}$ , while the addition of an anti-microbial preservative allowed electrodes to be used for up to 4 weeks, with only minimal loss in signal.<sup>30</sup>

**Binding Activity of Silicate-Immobilized scFv.** While the anti-domoic acid scFv has previously been demonstrated to bind its antigen in enzyme immunoassays,<sup>10</sup> in this work we investigated the binding ability—and stability of binding—of the silicate-immobilized scFv. The antibody fragment was found to bind its antigen on all supports. SBA-15 and MCM-41/80 exhibited very similar binding behavior, with the same rate of interaction between the adsorbed scFv and its antigen (Figure

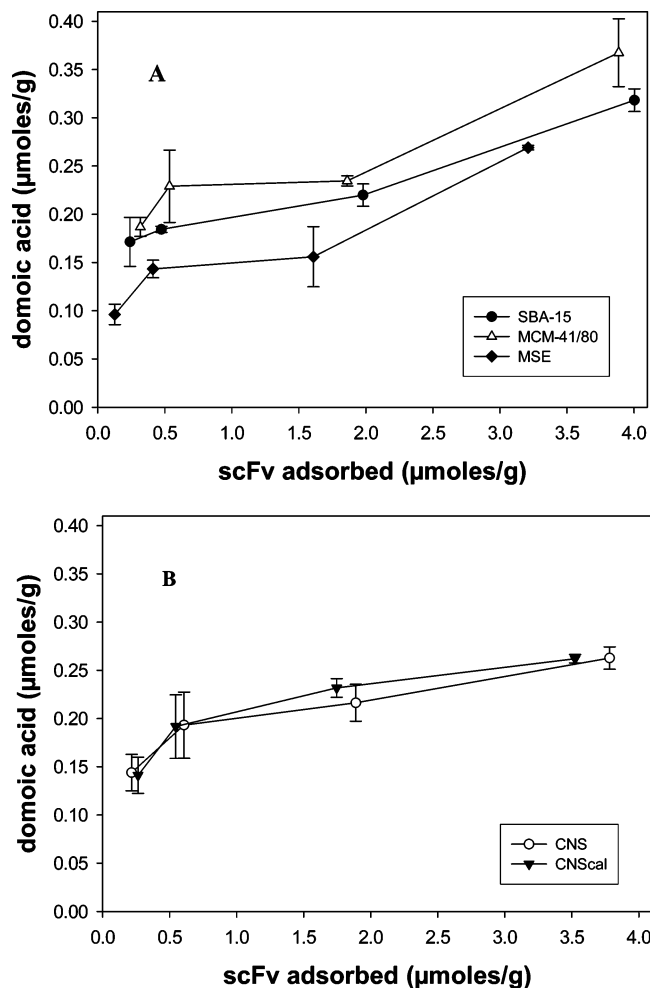


**Figure 4.** Domoic acid binding activity of scFv immobilized on (A) SBA-15, MCM-41/80, and MSE; and (B) CNS and CNScaI. Values are corrected for binding of domoic acid to silicates, and error bars represent standard deviations obtained from triplicate samples. The initial domoic acid concentration was 1  $\mu\text{g/mL}$ .

4A). MSE exhibited a weaker interaction with domoic acid but, like SBA-15 and MCM-41/80, had not reached saturation at 1  $\mu\text{g/mL}$  domoic acid and a 5  $\mu\text{M}$  initial scFv concentration. CNS and CNScaI showed behavior similar to each other but were close to saturated at 5  $\mu\text{M}$  incubated scFv (Figure 4B), indicating that, despite their larger pores, the surface area accessible for antibody adsorption in these materials is significantly less than that in MCM-41/80 and SBA-15. This form of saturation at a protein concentration considerably lower than that theoretically necessary to cover the surface has not previously been observed in our group in studies of the adsorption and activity of a variety of proteins on the present and other mesoporous supports.<sup>3,33,35,39</sup>

As it is not possible to precisely control the amount of scFv adsorbed onto the individual materials and so to compare directly the binding activity of each of the silicates, the amount of domoic acid bound by each material was normalized to take into account the concentration of adsorbed scFv. One domoic acid molecule was bound for every 1.3–1.9 scFv molecules at scFv concentrations less than 0.3  $\mu\text{mol/g}$  (Figure 5). This “specific activity” decreased steeply for all silicates with increasing concentration of adsorbed scFv, with a domoic acid:scFv ratio of 1:10 for all materials at scFv concentrations of 1.5  $\mu\text{mol/g}$  and higher (Figure 5). As little difference could be detected in the activity of the antibody fragment immobilized on the different materials, the major effect of the physicochem-

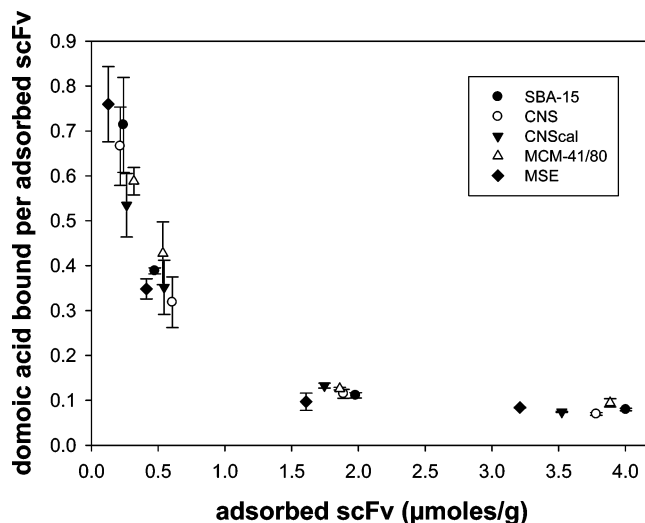


**Figure 5.** Specific activity (domoic acid bound/scFv concentration) of scFv adsorbed onto mesoporous materials. Error bars represent standard deviations obtained from triplicate samples. The initial domoic acid concentration was 1  $\mu\text{g/mL}$ , and binding was carried out at pH 7.4.

ical differences among the mesoporous supports was clearly on the efficiency of scFv adsorption.

It is clear from Figure 5 that the scFv is not as readily accessible to domoic acid at high adsorbed concentrations as at low scFv concentrations. As domoic acid ( $\text{C}_{15}\text{H}_{21}\text{N}_1\text{O}_6$ ) has a molecular mass of only 311 Da, its diffusion into and throughout the mesopores is unlikely to limit access, while the fact that only 10–12% of domoic acid was bound by the antibody in the presence of 3–4  $\mu\text{mol/g}$  adsorbed scFv (Figure 5) indicates that domoic acid was not limiting at the concentration used in the analysis. Thus, it appears that the scFv forms a multilayer on the mesoporous materials at high protein concentrations, rendering buried antibody molecules increasingly less accessible to domoic acid and resulting in the decrease in domoic acid:scFv seen in Figure 5. Based on surface area calculations outlined above, this multilayer exists at the surface and blocking rather than penetrating deeply into the pores. Similar effects of a protein multilayer on specific activity have been reported previously in studies with cytochrome *c*.<sup>39</sup> Here, the specific activity decreased rapidly with increasing cytochrome *c* concentration on a mesoporous material with pores smaller than the molecular diameter, while specific activity also decreased, albeit with a slower rate, on a support with pores sufficiently large for penetration of the protein molecules.

Of all the materials, MSE exhibits the lowest domoic acid binding, which correlates with it having the lowest amount of adsorbed scFv (Figures 2 and 3), due to its weaker interaction with the antibody fragment at the experimental pH. Its decreasing specific activity indicates that the support is saturated by 1.6  $\mu\text{mol/g}$  scFv, though this protein concentration should, theoretically, cover only approximately 1.4% of the available surface area. While SBA-15 is a pure silica material consisting of  $\text{SiO}_2$  units with  $\text{Si}-\text{OH}$  hydroxyl groups on the surface, MSE is a periodic mesoporous organosilane with  $-\text{CH}_2\text{CH}_2-$  groups interspersed periodically between  $\text{SiO}_2$  units. The presence of the  $-\text{CH}_2\text{CH}_2-$  moieties would be expected to lead to increased potential hydrophobic interactions with nonpolar patches on the adsorbed antibody fragment but weaker electrostatic-type interactions, so the interaction of MSE with the scFv and the reduced leakage upon desorption with PEG suggest that

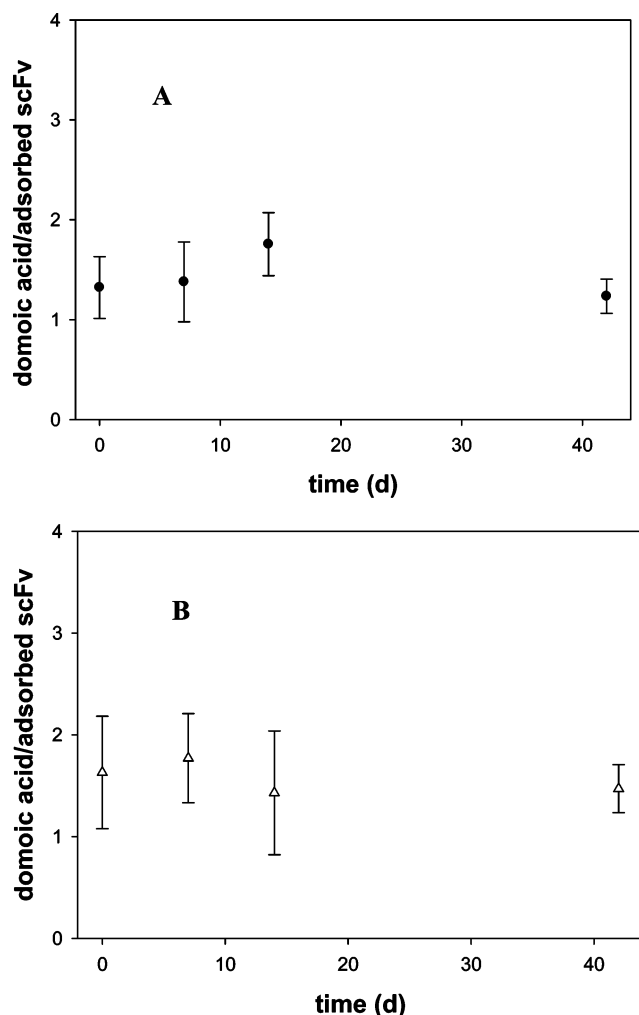


**Figure 6.** Plot of amount of domoic acid bound per scFv molecule as a function of time when immobilized on (A) SBA-15 and (B) MCM-41/80. scFv was adsorbed to each silicate at an initial concentration of 1  $\mu\text{mol/g}$ , followed by binding of domoic acid at 5  $\mu\text{g/mL}$ .

hydrophobic interactions are more dominant in mediating adsorption of the scFv to this material.

**Stability of Binding.** Following adsorption of 1  $\mu\text{M}$  scFv to MCM-41/80 and SBA-15, samples were stored at 4  $^{\circ}\text{C}$  and the domoic acid binding of the immobilized scFv was measured at intervals over a 42-day period. The analysis indicated that the scFv–silicate materials were stable during storage at 4  $^{\circ}\text{C}$ , with no significant reduction in their initial domoic acid binding ability after 42 days of storage (data not shown). Normalization of domoic acid binding for the concentration of scFv adsorbed to each material confirmed that the specific activity of the scFv remained unchanged (Figure 6), thus verifying that no significant leakage of the scFv occurred over the 42-day storage and that the binding activity of the silicates was also unaffected. This behavior is clearly within standard parameters for immunosensor stability, which indicate that sensor use should be continued only while binding capacity remains within 20% of original values.<sup>42</sup>

**Limit of Detection.** The E.U. and U.S.A. have set a regulatory upper limit for domoic acid in shellfish of 20  $\mu\text{g/g}$  to protect consumers from amnesic shellfish poisoning.<sup>21</sup> While this study was not designed to determine the lower limit of detection of the silicate-immobilized scFv, it is instructive, nonetheless, to consider whether such MPS materials might be

used to generate a sensor that could meet these regulatory requirements.

The antibody fragment adsorbed on SBA-15 and MCM-41/80 successfully detected 1  $\mu\text{g/mL}$  domoic acid in solution (Figure 4), which, based on published protocols for preparation of blue mussel tissue for domoic acid immunodetection,<sup>43</sup> corresponds to 20  $\mu\text{g/g}$  domoic acid in shellfish samples. Recovery was low in this study, with only 6–7% of domoic acid bound at adsorbed scFv concentrations from 0.5 to 2  $\mu\text{mol/g}$ , and 10–12% with 4  $\mu\text{mol/g}$  scFv (Figure 4). Nevertheless, the analysis indicates the potential use of mesoporous silicates in the development of a rapid, in situ detection method for domoic acid above safe levels. This preliminary in situ screening could then be followed by laboratory-based quantification of toxin levels using more accurate but labor-intensive methods such as immunoassays (limit of detection 0.025–0.04  $\mu\text{g/g}$ )<sup>28,43</sup> or HPLC-based methods such as LC/UV (0.6  $\mu\text{g/g}$ ),<sup>26</sup> LC with fluorimetric detection (6 ng/g),<sup>44</sup> LC/MS (0.1–0.2  $\mu\text{g/g}$ ),<sup>24,26</sup> or LC/MS/MS (0.02  $\mu\text{g/g}$ ).<sup>45</sup>

## Conclusions

This study represents the first detailed analysis of the adsorption and activity of a recombinant antibody fragment on mesoporous silicate materials. The scFv antibody fragment was immobilized onto mesoporous silicates of varying surface areas and pore diameters, but the isoelectric points of the antibody fragment and adsorbent material were found to be the most important determinant of protein adsorption. The antibody fragment was active on all materials and stably bound its antigen, domoic acid, in solution with a sensitivity sufficient to meet regulatory requirements. While the analysis was carried out with an antibody fragment specific for the neurotoxin domoic acid, the highly conserved domain architecture of antibody molecules and their derived fragments confer general relevance in scFv immobilization for sensor development.

**Acknowledgment.** X.H. and S.H. were funded by Grants ATRP/01/113 and SC/2003/159, respectively, from the Enterprise Ireland Science and Technology Development Agency. S.S. and S.W. were funded by Irish Research Council for Science, Engineering and Technology (IRCSET) Postdoctoral and Postgraduate Fellowships, respectively.

## References and Notes

- Beck, J. S.; Vartuli, J. C.; Roth, W. J.; Leonowicz, M. E.; Kresge, C. T.; Schmitt, K. D.; Chu, C. T. W.; Olson, D. H.; Sheppard, E. W.; McCullen, S. B.; Higgins, J. B.; Schlenker, J. L. *J. Am. Chem. Soc.* **1992**, *114*, 10834.
- Zhao, D.; Huo, Q.; Feng, J.; Chmelka, B. F.; Stucky, G. D. *J. Am. Chem. Soc.* **1998**, *120*, 6024.
- Deere, J.; Magner, E.; Wall, J. G.; Hodnett, B. K. *J. Phys. Chem. B* **2002**, *106*, 7340.
- Han, Y. J.; Stucky, G. D.; Butler, A. *J. Am. Chem. Soc.* **1999**, *121*, 9897.
- Diaz, J. F.; Balkus, K. J. *J. Mol. Catal. B* **1996**, *2*, 115.
- Washmon, L. L.; Balkus, K. J., Jr. *J. Mol. Catal. B* **2000**, *10*, 453.
- Holliger, P.; Hudson, P. *J. Nat. Biotechnol.* **2005**, *23*, 1126.
- Batra, S. K.; Jain, M.; Wittel, U. A.; Chauhan, S. C.; Colcher, D. *Curr. Opin. Biotechnol.* **2002**, *13*, 603.
- Backmann, N.; Zahnd, C.; Huber, F.; Bietsch, A.; Plückthun, A.; Lang, H. P.; Güntherodt, H. J.; Hegner, M.; Gerber, C. *Proc. Natl. Acad. Sci. U.S.A.* **2005**, *102*, 14587.
- Hu, X.; O'Dwyer, R.; Wall, J. G. *J. Biotechnol.* **2005**, *120*, 38.
- Bates, S. S.; Bird, C. J.; Defreitas, A. S. W.; Foxall, R.; Gilgan, M.; Hanic, L. A.; Johnson, G. R.; McCulloch, A. W.; Odense, P.; Pocklington, R.; Quilliam, M. A.; Sim, P. G.; Smith, J. C.; Rao, D. V. S.; Todd, E. C. D.; Walter, J. A.; Wright, J. L. C. *Can. J. Fish. Aquat. Sci.* **1989**, *46*, 1203.
- Jeffery, B.; Barlow, T.; Moizer, K.; Paul, S.; Boyle, C. *Food Chem. Toxicol.* **2004**, *42*, 545.

- (13) Subba Rao, D. V.; Quilliam, M. A.; Pocklington, R. *Can. J. Fish. Aquat. Sci.* **1988**, *45*, 2076.
- (14) Mos, L. *Environ. Toxicol. Pharmacol.* **2001**, *9*, 79.
- (15) Perl, T. M.; Bedard, L.; Kosatsky, T.; Hockin, J. C.; Todd, E. C.; Remis, R. S. *N. Engl. J. Med.* **1990**, *322*, 1775.
- (16) Rhodes, L.; Scholin, C.; Garthwaite, I. *Nat. Toxins* **1998**, *6*, 105.
- (17) Amzil, Z.; Fresnel, J.; Le Gal, D.; Billard, C. *Toxicon* **2001**, *39*, 1245.
- (18) Sierra Beltran, A.; Palafox-Urbe, M.; Grajales-Montiel, J.; Cruz-Villacorta, A.; Ochoa, J. L. *Toxicon* **1997**, *35*, 447.
- (19) Lefebvre, K. A.; Bargu, S.; Kieckhefer, T.; Silver, M. W. *Toxicon* **2002**, *40*, 971.
- (20) Scholin, C. A.; Gulland, F.; Doucette, G. J.; Benson, S.; Busman, M.; Chavez, F. P.; Cordaro, J.; DeLong, R.; De Vogelaere, A.; Harvey, J.; Haulena, M.; Lefebvre, K.; Lipscomb, T.; Loscutoff, S.; Lowenstine, L. J.; Marin, R., III; Miller, P. E.; McLellan, W. A.; Moeller, P. D.; Powell, C. L.; Rowles, T.; Silvagni, P.; Silver, M.; Spraker, T.; Trainer, V.; Van Dolah, F. M. *Nature* **2000**, *403*, 80.
- (21) Iverson, F.; Truelove, J. *Nat. Toxins* **1994**, *2*, 334.
- (22) Yasumoto, T.; Murata, M.; Oshima, Y.; Matsumoto, G. K.; Clardy, J. Diarrhetic shellfish poisoning. In *Seafood Toxins*; Ragelis, E. P., Ed.; ACS Symposium Series 262; American Chemical Society: Washington, DC, 1984; pp 207–214.
- (23) Quilliam, M. A. *J. AOAC Int.* **1995**, *78*, 555.
- (24) Lawrence, J. F.; Lau, B. P.; Cleroux, C.; Lewis, D. J. *Chromatogr.* **1994**, *659*, 119.
- (25) Tor, E. R.; Puschner, B.; Whitehead, W. E. *J. Agric. Food Chem.* **2003**, *51*, 1791.
- (26) López-Rivera, A.; Suárez-Isla, B. A.; Eilers, P. P.; Beaudry, C. G.; Hall, S.; Fernandez Amandi, M.; Furey, A.; James, K. J. *Anal. Bioanal. Chem.* **2005**, *381*, 1540.
- (27) Smith, D. S.; Kitts, D. D. *J. Agric. Food Chem.* **1995**, *43*, 367.
- (28) Kawatsu, K.; Hamano, Y.; Noguchi, T. *Toxicon* **1999**, *37*, 1579.
- (29) Kreuzer, M. P.; Pravda, M.; O'Sullivan, C. K.; Guilbault, G. G. *Toxicon* **2002**, *40*, 1267.
- (30) Micheli, L.; Radoi, A.; Guarrina, R.; Massaud, R.; Bala, C.; Moscone, D.; Palleschi, G. *Biosens. Bioelectron.* **2004**, *20*, 190.
- (31) Ge, L.; Knappik, A.; Pack, P.; Freund, C.; Plückthun, A. Expressing antibodies in *Escherichia coli*. In *Antibody Engineering*, 2nd ed.; Borrebaeck, C. A. K., Ed.; Oxford University Press: New York, 1995; pp 229–266.
- (32) Zhao, D.; Feng, J.; Huo, Q.; Melosh, N.; Fredrickson, G. H.; Chmelka, B. F.; Stucky, G. D. *Science* **1998**, *279*, 548.
- (33) Deere, J.; Magner, E.; Wall, J. G.; Hodnett, B. K. *Chem. Commun.* **2001**, *5*, 465.
- (34) Bao, X. Y.; Zhao, X. S.; Li, X.; Chia, P. A.; Li, J. J. *Phys. Chem. B* **2004**, *108*, 4684.
- (35) Hudson, S.; Magner, E.; Cooney, J.; Hodnett, B. K. *J. Phys. Chem. B* **2005**, *109*, 19496.
- (36) Kresge, C. T.; Leonowicz, M. E.; Roth, W. J.; Vartuli, J. C.; Beck, J. S. *Nature* **1992**, *359*, 710.
- (37) Barrett, E. P.; Joyner, L. G.; Halenda, P. P. *J. Am. Chem. Soc.* **1951**, *73*, 373.
- (38) Brunauer, S.; Emmett, P. H.; Teller, E. *J. Am. Chem. Soc.* **1938**, *60*, 309.
- (39) Deere, J.; Magner, E.; Wall, J. G.; Hodnett, B. K. *Catal. Lett.* **2003**, *85*, 19.
- (40) Deere, J.; Serantoni, M.; Edler, K.; Hodnett, B. K.; Wall, J. G.; Magner, E. *Langmuir* **2004**, *20*, 532.
- (41) Suh, C. W.; Kim, M. Y.; Choo, J. B.; Kim, J. K.; Kim, H. K.; Lee, E. K. *J. Biotechnol.* **2004**, *112*, 267.
- (42) Wong, R. L.; Mytych, D.; Jacobs, S.; Bordens, R.; Swanson, S. J. *J. Immunol. Methods* **1997**, *209*, 1.
- (43) Yu, F. Y.; Liu, B. H.; Wu, T. S.; Chi, T. F.; Su, M. C. *J. Agric. Food Chem.* **2004**, *52*, 5334.
- (44) James, K. J.; Gillman, M.; Lehane, M.; Gago-Martinez, A. *J. Chromatogr., A* **2000**, *871*, 1.
- (45) McNabb, P.; Selwood, A. I.; Holland, P. T.; Aasen, J.; Aune, T.; Eaglesham, G.; Hess, P.; Igarishi, M.; Quilliam, M.; Slattery, D.; Van de Riet, J.; Van Egmond, H.; Van den Top, H.; Yasumoto, T. *J. AOAC Int.* **2005**, *88*, 761.